Photosystem I

Norbert Krauß, *Freie Universität Berlin, Berlin, Germany*
Wolfram Saenger, *Freie Universität Berlin, Berlin, Germany*

Secondary article

Article Contents

In oxygenic photosynthesis, the two protein–pigment complexes photosystem I and photosystem II are involved in the light-driven charge separation across the thylakoid membrane, which results in the oxidation of water to O_2 and in the reduction of $NADP^+$ to NADPH. In addition to a photosynthetic reaction centre, each of these photosystems contains a core antenna system. The crystal structure of photosystem I reveals the spatial organization of protein subunits and cofactors.

Introduction: Oxygenic Photosynthesis

In plants, algae and photosynthetic bacteria, there is a large group of light-energy driven reaction centres engaged in both anoxygenic and oxygenic photosynthesis. Oxygenic photosynthesis is associated with two protein–pigment complexes, photosystems I and II (PS I and PS II), which convert the energy of absorbed solar light into chemical energy and produce molecular oxygen, O_2, as a side product. PS I and PS II are located in the photosynthetic thylakoid membranes of cyanobacteria, algae and higher plants. They represent archetypal members of two families of photosynthetic systems characterized by their intrinsic terminal electron acceptors, iron–sulfur cluster (type I; PS I) or quinone (type II; PS II).

In PS I and PS II, large chlorophyll-based and carotenoid-based antenna systems absorb solar light and channel the energy to a primary electron donor P consisting of a pair of chlorophyll molecules located near the luminal side of the membrane-integral protein subunits. After excitation of P to P*, an electron is transferred to the primary electron acceptor A, yielding the radical pair $P^+\dot{A}-$. This initial charge separation is followed by a series of individual electron transfer steps along the cofactors of the electron transfer chain (ET chain) towards the stromal side of the membrane.

During a photosynthetic reaction cycle, PS II and PS I are linked in series. The primary electron donor of PS II, P680, is excited by light, followed by the initial charge separation, which leaves the oxidized donor $P680^+$, providing a highly positive redox potential used in the oxidation of water with subsequent release of O_2 and H^+. The ET chain guides the electrons to the stromal side of the thylakoid membrane. PS II is linked to PS I through a pool of plastoquinone molecules, the cytochrome b_6/f complex and either plastocyanin or cytochrome c_6, which transfer electrons to the luminal side of PS I. Here, light excites the primary donor P700 and initiates transfer of an electron to the stromal side of PS I, where it is donated from the terminal acceptor, an Fe_4S_4 cluster, to either ferredoxin or flavodoxin, which finally transport the electron to $NADP^+$ (oxidized form of nicotinamide–adenine dinucleotide phosphate) reductase to produce NADPH (reduced form). The vectorial electron transfer of PS I and PS II gives rise to a transmembrane electrochemical potential that drives ATP (adenosine triphosphate) synthesis. Both ATP and NADPH are utilized in a series of dark reactions to reduce CO_2 to carbohydrates.

Structure and Function of Biological Macromolecules Are Closely Related

Since the biochemical and physical functions of a biological macromolecule are tightly coupled to its three-dimensional structure, they can only be understood at the atomic level if the structure is known. For this reason, PS I from different organisms was crystallized, but only the crystals obtained from the thermophilic cyanobacterium *Synechococcus elongatus* proved suitable for high-resolution structure determination by X-ray diffraction (Fromme and Witt, 1998). The crystals of PS I from the other (mesophilic) organisms obtained so far have been either too small and/or imperfect and did not show high-resolution X-ray diffraction.

Global Description of Cyanobacterial PS I

PS I of cyanobacteria consists of 11 protein subunits denoted PsaA to PsaF and PsaI to PsaM according to their gene names. The essential features of these subunits such as position in the membrane or on the stromal/luminal side, molecular mass and number of transmembrane α helices, as well as a schematic description of the electron transfer chain, are shown in **Table 1** and **Figure 1**.

The two large subunits PsaA and PsaB (83 kDa each) are structurally homologous and are related to each other by a pseudo-C_2 rotation noncrystallographic axis oriented

Table 1 Protein subunits of cyanobacterial PS I

Subunit name	Molecular mass (kDa)	Predicted number of transmembrane α helices	Comments
PsaA	83	11	Binds membrane intrinsic electron transfer (ET) chain and majority of core antenna cofactors together with PsaB
PsaB	83	11	Binds membrane intrinsic ET chain and majority of core antenna cofactors together with PsaA
PsaC	9	0	Located on the stromal side, binds iron–sulfur clusters F_A and F_B
PsaD	15	0	Located on the stromal side, involved in ferredoxin/flavodoxin docking
PsaE	8	0	Located on the stromal side, involved in ferredoxin/flavodoxin docking and cyclic electron flow
PsaF	15	1–2	Involved in plastocyanin/cytochromec_6 docking
PsaI	4	1	Stabilizes PsaL in the PS I complex
PsaJ	5	1	Stabilizes PsaF in the PS I complex
PsaK	8	2	Function unknown
PsaL	16	2–3	Responsible for PS I trimerization
PsaM	3	1	Function unknown

normally to the membrane plane and located between the two subunits. The electron transfer chain (ET chain) is arranged along this pseudo-C_2 symmetry axis and comprises six chlorophyll and two phylloquinone molecules together with three Fe_4S_4 clusters. Nine of these cofactors of the ET chain, the organic molecules and the Fe_4S_4 cluster are bound to PsaA and PsaB; only the two terminal electron acceptors, the Fe_4S_4 clusters F_A and F_B, are coordinated to subunit PsaC on the stromal side of PS I, flanked by subunits PsaD and PsaE. The other small subunits (4–16 kDa) are located in the membrane, spanning it with one or two transmembrane α helices. A total of 83 core antenna Chl *a* were identified in the crystal structure at 4 Å resolution, but the 20–25 carotenoids known to be associated with the PS I monomer could not be located in the electron density map. The total molecular mass of the PS I monomer is 340 kDa. In the crystals (and probably in the thylakoid membrane), PS I from *Synechococcus elongatus* occurs as homotrimer. The three monomers are in contact through transmembrane subunits PsaI and PsaL located close to and symmetry related by a (crystallographic) C_3 axis. They form a clearly defined 'connection domain'.

Structural Details of *Synechococcus elongatus* PS I

Amino acid sequences suggest hydrophobic stretches

The amino acid sequences of the 11 subunits of *Synechococcus elongatus* PS I were derived on the basis of the corresponding gene sequences (Mühlenhoff *et al*., 1993). The two large subunits PsaA and PsaB have remarkably similar sequences, with 47% identity, suggesting that they have a common origin. The sequences of all the other subunits are unrelated in sequences and lengths of the polypeptide chains. Hydrophobicity plots show that most of the nine small subunits (except for the stromally located PsaC, PsaD, PsaE) contain one or two larger hydrophobic segments. For the large subunits PsaA and PsaB, these plots are very similar, with 11 hydrophobic segments each. In analogy to the known structures of purple bacterial reaction centres (PbRC) and other membrane proteins, it can be expected that all the longer hydrophobic segments are folded into α helices spanning the thylakoid membrane.

The two large subunits PsaA and PsaB are related by a pseudo-C_2 axis

The electron density map shows that within the inner-membrane space the protein subunits fold into α helical structures, as shown so far for the majority of membrane

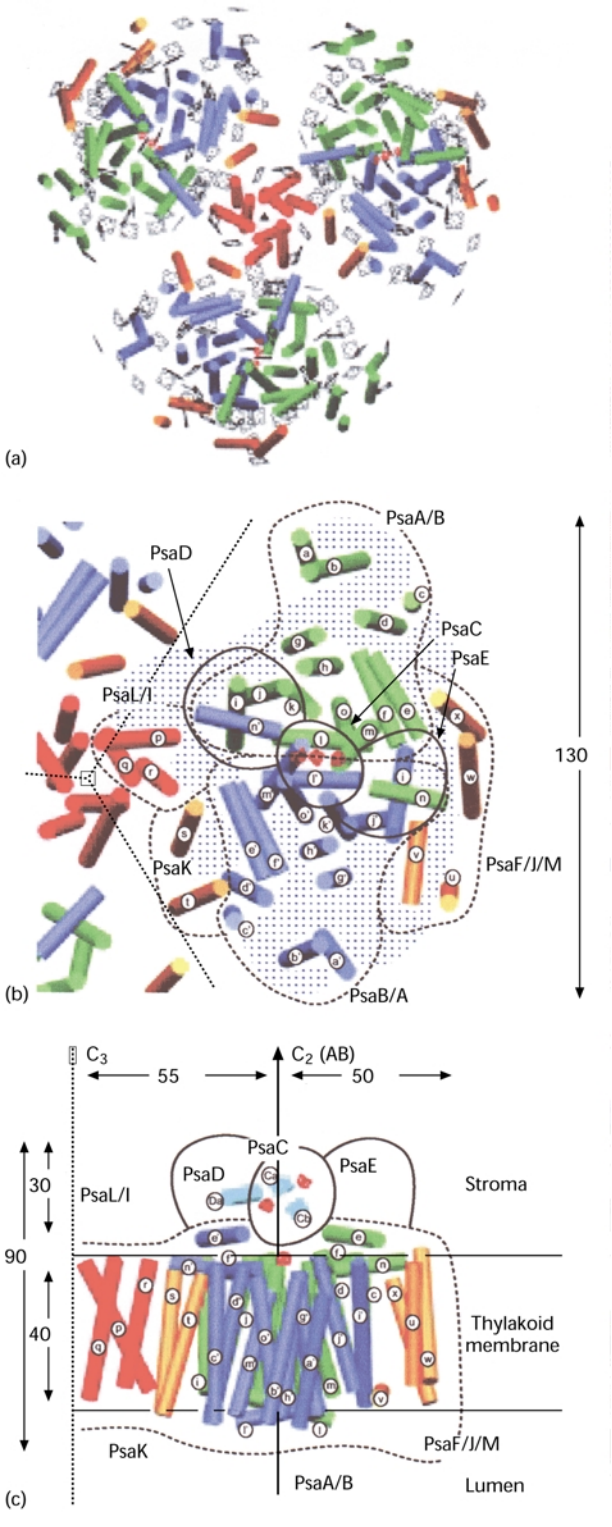

protein structures. At 4 Å resolution it is impossible to identify individual amino acid side-chains, and usually the backbones of the polypeptide chains cannot be traced completely. Therefore, the transmembrane α helices can only tentatively be assigned to the eight membrane-intrinsic subunits of PS I, taking into account the number of transmembrane α helices predicted for each subunit from hydrophobicity analyses (**Table 1**) and using all the available biochemical and biophysical data on the spatial architecture of PS I. These data resulted mainly from mutagenesis, electron microscopy and chemical cross-linking studies.

The two large subunits with high sequence similarity form a pseudosymmetric PsaA/PsaB heterodimer. The pseudo-C_2 axis, which relates both subunits to each other, is normal to the membrane plane and passes right through the Fe_4S_4 cluster F_X.

The 2×11 transmembrane α helices of PsaA and PsaB are denoted as a–d, g–k, o, m and as a′–d′, g′–k′, o′, m′ in **Figure 1**. There are four additional shorter α helices in each large subunit; three are located on the stromal side of PS I (e, f, n and e′, f′, n′) and one is on the luminal side (l and l′). These α helices are parallel to and positioned on the surface of the membrane plane.

In PsaA and PsaB, the 11 transmembrane α helices are divided into a C-terminal 'core antenna domain' defined by α helices a–h and a′–h′ and an N-terminal 'reaction centre domain' containing α helices i–o and i′–o′.

Distribution of the small subunits in the structure of PS I

The most obvious of the small subunits are the stromally located PsaC, PsaD and PsaE (**Figure 1c**). They do not contain long hydrophobic segments; in PsaC there are two short α helices similar to bacterial two- Fe_4S_4 ferredoxin; in PsaE a five-stranded β barrel is found, as also shown by NMR spectroscopy (Falzone *et al.*, 1994); PsaD contains one α helix and a short β sheet (Klukas *et al.*, 1999a). All the

Figure 1 Overall structure of PS I. (a) Structural model of the PS I trimer, including the identified α helices (represented by cylinders) except those of PsaC and PsaD, the Chl *a* of the core antenna system and the Chl *a* and the phylloquinone cofactors of the ET chain. The Fe_4S_4 clusters are shown as red cubes. View from the stromal side of the thylakoid membrane. (b) Arrangement of the α helices of one PS I monomer, shown with parts of the adjoining monomers (separated by bold, broken lines), and tentative assignment of the membrane intrinsic subunits. View as in (a), s marks the C_3 symmetry axis of the PS I trimer. The two sets of α helices related by the pseudo-C_2 symmetry axis of the PsaA/PsaB heterodimer are labelled a to o (green) and a′ to o′ (blue), respectively. The region occupied by the Chl *a* of the PS I core antenna is indicated by light grey shading (dots). α Helices of the stromal subunits PsaC and PsaD have been omitted for clarity. (c) Side view, parallel to the membrane, of the arrangement shown in (b), but including the α helices of the stromal subunits PsaC and PsaD. The pseudo-C_2 axis of PsaA/PsaB is labelled C_2(AB); the crystallographic C_3 symmetry axis of the PS I trimer is denoted C_3 (modified from Schubert *et al.*, 1997).

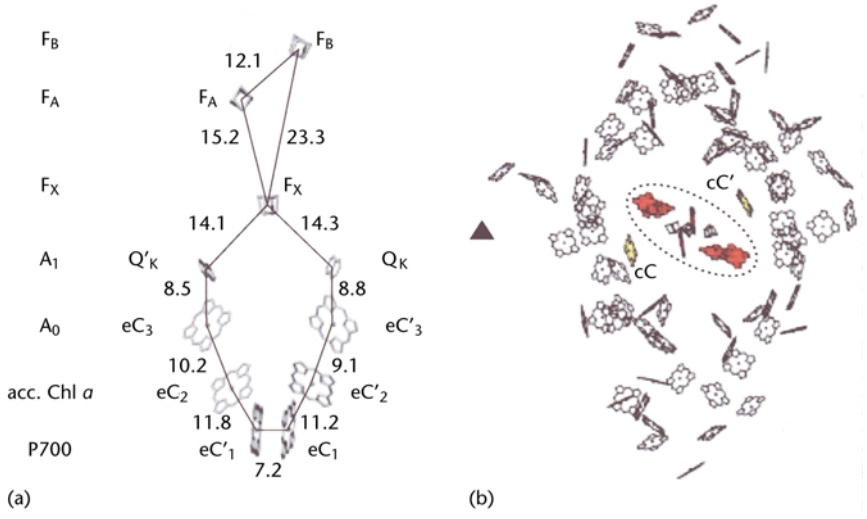

Figure 2 Arrangement of the PS I cofactors. (a) Cofactors of the ET chain with centre-to-centre distances (Å) and assignments to the spectroscopically identified cofactors are indicated; acc. Chl *a* are the accessory Chl *a*. View parallel to the membrane plane. (b) Complete set of 89 chlorophyll cofactors of the core antenna and the ET chain identified in the structure of PS I, are shown together with the three iron–sulfur clusters. Chlorophyll molecules of the ET chain (marked by broken line) are coloured red and 'connecting' Chl *a* cC and cC′ are yellow, iron sulfur clusters are shown as grey cubes. View perpendicular to the membrane plane from the stromal side, s marks the C_3 axis of the PS I trimer.

other small subunits are folded into one or two transmembrane α helices, and there is no significant formation of β sheet structure.

For some of the small subunits the function is clearly indicated. Since PsaC carries the two Fe_4S_4 clusters F_A and F_B, it is engaged in electron transfer between F_X and the carriers flavodoxin or Fe_2S_2-type ferredoxin. The docking site for these carriers on PS I is presumably formed by an indentation close to PsaC and between PsaD, PsaE, removed from (distal to) the C_3 axis (Klukas *et al*., 1999a; Lelong *et al*., 1996; Mühlenhoff *et al*., 1996).

For two other subunits, PsaI and PsaL, the function can be derived from their location close to the C_3 axis of the PS I trimer. According to the proposed assignment, Psa I contains one and PsaL two transmembrane α helices that pack tightly against each other and against the symmetry-related PsaI and PsaL to form a 'connection domain'. This view is corroborated by mutational studies showing that PsaI is required for stabilization of PsaL. Subunits PsaF and PsaJ are also close together at the outer periphery of the PSI trimer, where also PsaM might be located. The location of PsaK close to the 'connection domain' was proposed by exclusion. The function of the latter four small subunits is less clear than that of PsaC, PsaI and PsaL, but their location at the outer periphery of the PS I trimer suggests that they might stabilize and protect the core antenna system (Schubert *et al*., 1997).

The electron transfer chain

The electron transfer chain is responsible for the central function of PS I, which, biochemically, might be considered as that of a light-driven oxidoreductase: catalysis of the oxidation of plastocyanin or cytochrome c_6 docking at surface α helices l, l′ on the luminal side of PS I and close to P700, and the reduction of Fe_2S_2-type ferredoxin or flavodoxin at the stromal side, docking close to PsaC. Catalysis is achieved by light-induced transmembrane charge separation along the group of redox-active cofactors located around the pseudo-C_2 axis and spanning the thylakoid membrane – the electron transfer (ET) chain (**Figure 2**). Spectroscopic data and biochemical analyses have identified the primary electron donor P700 as a dimer of chlorophyll molecules, a chlorophyll monomer as primary acceptor A_0, and the phylloquinone (vitamin K_1) as secondary acceptor A_1. The Fe_4S_4 cluster F_X is coordinated to two cysteines each of PsaA and PsaB and located between these two subunits, right on the pseudo-C_2 axis. It forms an obtuse triangle with clusters F_A and F_B, which are coordinated by the stromal subunit PsaC.

From the electron density map it is not clear which of the two Fe_4S_4 clusters bound to PsaC is the spectroscopically identified cluster F_A and which is F_B. Recent data obtained by different groups indicate that the correct assignment is as shown in **Figure 2**, i.e. F_A is the proximal and F_B the distal cluster as seen from F_X, and the sequence of electron transfer is $F_X \rightarrow F_A \rightarrow F_B \rightarrow$ ferredoxin/flavodoxin.

Because of the relatively low resolution (4 Å) of the electron density map, the chlorophyll molecules could only be modelled as symmetric porphyrin molecules without ring substituents and without the fifth ring carrying the keto group. For the phylloquinone molecules, only their centre positions and the orientations of the long molecular axes of the naphthoquinone head groups were determined tentatively. The primary donor P700 consists of two pseudosymmetrically arranged chlorophyll molecules with roughly parallel porphyrin planes; the short plane-to-plane distance (3.8 ± 0.5 Å) could indicate a strong excitonic coupling contributing to the observed spectroscopic properties of P700. Like the two chlorophyll molecules eC_1 and eC_1' constituting P700, the other chlorophyll and quinone cofactors of the ET chain form two branches, where the Chl *a* monomers eC_2 and eC_3 as well as the position of the phylloquinone Q_K are related by the pseudo-C_2-axis to eC_2' and eC_3' and the position of Q_K', respectively. Spectroscopically identified A_0 might be identical with eC_3 or eC_3', whereas A_1 could be Q_K or Q_K'. As a consequence of these assignments, eC_2 and eC_2', located at intermediate positions between pairs eC_1, eC_1' and eC_3, eC_3', would correspond to cofactors of the ET chain that have not been identified spectroscopically.

According to a simplified approach to Marcus' theory of electron transfer proposed by Moser, Dutton and co-workers, the 'optimal rate' of intraprotein electron transfer can be calculated if the 'edge-to-edge distance', i.e. the shortest distance between those atoms of the donor and acceptor that are involved in the reaction, is known. The rate for the electron transfer from P700 to A_0 is several orders of magnitudes higher than expected from the relatively long 'edge-to-edge distance' between these cofactors, as they were determined from the PS I structure (Klukas *et al*., 1999b). Probably eC_2 or eC_2' takes part in electron transfer as an intermediate electron acceptor between P700 and A_0. These cofactors were called 'accessory chlorophyll' molecules (**Figure 2a**)because of their analogy to the 'accessory bacteriochlorophyll' molecules found in the structures of PbRC, which belong to the group of type II reaction centres. The other kinetic data determined for forward electron transfer along the chain are compatible with the distances between the respective cofactors. In contrast to PbRC, where electron transfer is unidirectional along one active branch of the electron transfer chain, it is not clear whether electron transfer is uni- or bidirectional in PS I. Within the error limits, the structure analysis at 4 Å resolution does not reveal symmetry-breaking elements for the ET chain within the membrane-intrinsic region of PS I.

The ET chain is enclosed by a palisade of 2×5 transmembrane α helices belonging to the C-termini of PsaA and PsaB (**Figure 1**) and arranged around the pseudo-C_2 axis. The palisade α helices (i, j, k, m, o and i′, j′, k′, m′, o′) clearly separate the cofactors of the ET chain from those of the core antenna system. There are only two Chl *a* structurally linking ET chain and core antenna ('connecting' Chl *a* cC and cC′ shown yellow in **Figure 2**). They are possibly required for transmission of light energy from the antenna to the P700 cofactors eC_1 and eC_1' via eC_3 and eC_2 (or via eC_3' and eC_2') (Schubert *et al*., 1997).

The core antenna

Photosynthetic organisms use a variety of antenna complexes to increase the spectral bandwidth of light absorption as well as the absorption cross-section. Among the different antenna complexes one may distinguish between external antennae, which are only associated with a photosynthetic reaction centre, and core antennae, which are internal components of a photosystem. PS I binds ~100 Chl *a* molecules, the majority of which (except for six chlorophylls that are part of the ET chain) constitute the core antenna system together with ~15–25 carotenoid molecules. The carotenoids could not be identified in the electron density map, but 83 antenna Chl *a* molecules were modelled as symmetric porphyrin molecules (**Figure 2**).

The Chl *a* of the core antenna system of PS I are arranged in a space best described as a hollow, elliptical cylinder that narrows slightly towards the luminal side. It surrounds the ET chain and the palisade of α helices (i, j, k, m, o and i′, j′, k′, m′, o′) and α helices g, h and g′, h′ from PsaA and PsaB. The outer rim of the cyclindrical space is formed by α helices a–d and a′–d′ of the large subunits and by α-helices p–u and w of the small membrane-intrinsic subunits (except for the stromal PsaC, PsaD and PsaE).

Each Chl *a* of the core antenna has at least one neighbour within a centre-to-centre distance of 16 Å. If all Chl *a* within distances ≤ 16 Å are connected, a net is formed that is clearly divided into four clusters mutually linked by only one or two Chl *a*. The core antenna roughly exhibits pseudo-C_2 symmetry similar to that described for PsaA and PsaB, suggesting that these two subunits carry most of the antenna Chl *a*. There are only few Chl *a* near the threefold axis, probably coordinated by the connecting domain subunits PsaI and PsaL. Within the PS I trimer, the closest centre-to-centre distances between Chl *a* of adjacent monomers are 23–25 Å, significantly longer than those ≤ 16 Å within the core antenna. This suggests that there is only slow transfer of energy between the PS I monomers.

Comparison of PS I with other photosynthetic reaction centres

The known three-dimensional structures of PS I and of PbRC allow similarities in their architecture to be deduced, and comparison of amino acid sequences suggests a prediction of the structure of PS II, for which the most detailed information is available from the structural model of a PS II core complex determined at 8 Å resolution (Rhee *et al*., 1998).

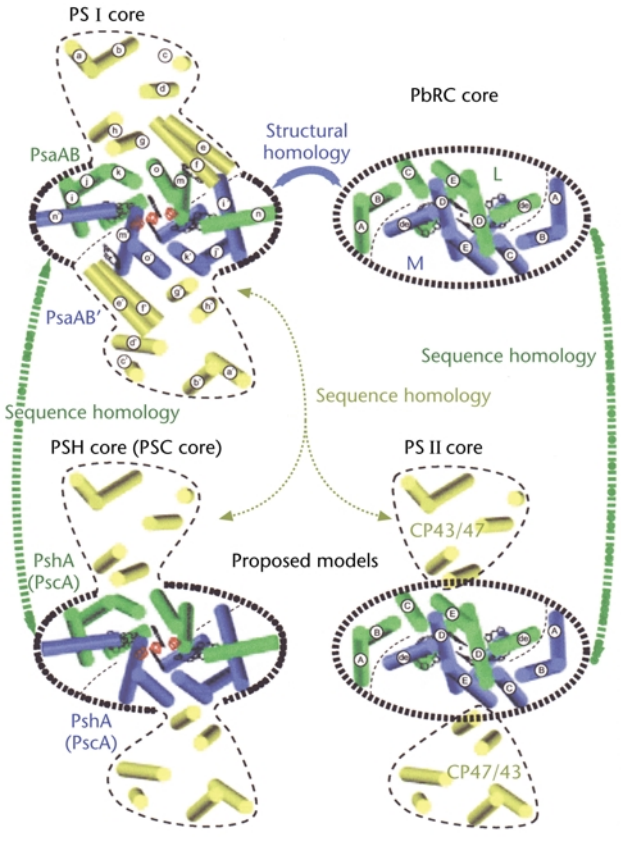

Figure 3 Proposed structural models for the core structures of heliobacterial PSH, green sulfur bacterial PSC and cyanobacterial or higher plant PS II on the basis of the structures of PS I and PbRC and known sequence similarities (from Schubert *et al.*, 1998).

The amino acid sequences of several subunits of PS II show considerable homology both with PbRC and with PS I. Comparison of sequences of PS II with PbRC suggests that the inner palisades of α helices surrounding the electron transfer chains (which are closely related in cofactor composition) are also structurally similar; conversely, there is homology between the sequences of antenna subunits CP43 and CP47 of PS II, containing six hydrophobic stretches, and the N-terminal halves of the large subunits PsaA and PsaB of PS I including the six transmembrane α helices a, b, c, d, g, h and a′, b′, c′, d′, g′, h′.

Like the L (light) and M (medium) subunits of PbRC, the inner core of PS I binding the membrane-intrinsic part of the ET chain consists of 10 transmembrane α helices, formed by the five C-terminal hydrophobic stretches each of PsaA and PsaB. The structures of the reaction centre cores of PbRC and PS I are strikingly similar, although there is only little sequence similarity between them.

By combining this information from the three-dimensional structures of PS I and PbRC and from the amino acid sequences of PS I, PS II and PbRC, it was possible to derive the model for the PS II complex D1–D2–CP43–CP47 shown in **Figure 3** (Schubert *et al.*, 1998). In this model, the other PS II subunits are not included because they do not show any significant sequence homology with the subunits of PS I or PbRC. Using the same arguments, the core structures of heliobacterial (PSH) and green sulfur bacterial (PSC) photosystems and PS I, which belong to the group of type I reaction centres, are expected to be similar because of sequence homology of their core subunits.

These studies suggest that photosynthetic systems of anoxygenic (PbRC, PSC and PSH as representatives) and oxygenic photosynthesis (PS I and PS II) have a common ancestor.

References

Falzone CJ, Kao YH, Zhao J, Bryant DA and Lecomte JTL (1994) Three-dimensional solution structure of PsaE from the cyanobacterium *Synechococcus* sp. strain PCC 7002, a photosystem I protein that shows structural homology with SH3 domains. *Biochemistry* **33**: 6052–6062.

Fromme P and Witt HT (1998) Improved isolation and crystallization of photosystem I for structural analysis. *Biochimica et Biophysica Acta* **1365**: 175–184.

Klukas O, Schubert WD, Jordan P *et al.* (1999a) Photosystem I, an improved model of the stromal subunits PsaC, PsaD and PsaE. *Journal of Biological Chemistry* **274**: 7351–7360.

Klukas O, Schubert WD, Jordan P *et al.* (1999b) Localization of two phylloquinones, Q_K and $Q_{K'}$, in an improved electron density map of photosystem I at 4 Å resolution. *Journal of Biological Chemistry* **274**: 7361–7367.

Lelong C, Boekema E, Kruip J *et al.* (1996) Characterization of a redox active cross-linked complex between cyanobacterial photosystem I and soluble ferredoxin. *EMBO Journal* **15**: 101–109.

Mühlenhoff U, Haehnel W, Witt HT and Herrmann RG (1993) Genes encoding eleven subunits of photosystem I from the thermophilic cyanobacterium *Synechococcus* sp. *Gene* **127**: 71–78.

Mühlenhoff U, Kruip J, Bryant DA *et al.* (1996) Characterization of a redox-active cross-linked complex between cyanobacterial photosystem I and its physiological acceptor flavodoxin. *EMBO Journal* **15**: 488–497.

Rhee KH, Morris EP, Barber J and Kühlbrandt W (1998) Three-dimensional structure of the plant photosystem II reaction centre at 8 Å resolution. *Nature* **396**: 283–286.

Schubert WD, Klukas O, Krauß N *et al.* (1997) Photosystem I of *Synechococcus elongatus* at 4 Å resolution: comprehensive structure analysis. *Journal of Molecular Biology* **272**: 741–769.

Schubert WD, Klukas O, Saenger W *et al.* (1998) A common ancestor for oxygenic and anoxygenic photosynthetic systems: a comparison based on the structural model of photosystem I. *Journal of Molecular Biology* **280**: 297–314.

Further Reading

Brettel K (1997) Electron transfer and arrangement of the redox cofactors in photosystem I. *Biochimica et Biophysica Acta* **1318**: 322–373.

Chitnis PR, Xu Q, Chitnis VP and Nechushtai R (1995) Function and organization of photosystem I polypeptides. *Photosynthesis Research* **44**: 23–40.

Golbeck JH (1994) Photosystem I in cyanobacteria. In: Bryant DA (ed.) *The Molecular Biology of Cyanobacteria*, pp. 319–360. Dordrecht: Kluwer Academic.

Golbeck JH (1999) A comparative analysis of the spin state distribution of *in vitro* and *in vivo* mutants of PsaC. *Photosynthesis Research* **61**: 107–144.

Lancaster CRD, Ermler U and Michel H (1995) The structures of photosynthetic reaction centers from purple bacteria as revealed by X-ray crystallography. In: Blankenship RE *et al.* (eds) *Anoxygenic Photosynthetic Bacteria*, pp. 503–526. Dordrecht: Kluwer Academic.

Marcus RA and Sutin N (1985) Electron transfers in chemistry and biology. *Biochimica et Biophysica Acta* **811**: 265–322.

Moser CC, Keske JM, Warncke K, Farid RS and Dutton PL (1992) Nature of biological electron transfer. *Nature* **355**: 796–802.